Model and Controller Reduction for Flexible Aircraft Preserving Robust Performance

Nabil Aouf, Benoit Boulet, *Member, IEEE*, and Ruxandra Botez

***Abstract*—This paper presents a systematic model/controller order reduction method applied to flexible aircraft. The method, based on mixed μ-synthesis, determines which flexible modes can be truncated from the full-order model of the aircraft and finds a corresponding reduced order controller preserving robust closed-loop performance. This method is of interest for practical model and controller reduction for flexible aircraft because in this context it is important to keep the physical interpretation of the truncated and remaining modes. Numerical examples are given for a flexible model of a B-52 bomber and for a three-mass flexible system.**

***Index Terms*—Aerospace control, aircraft control, flexible aircraft, flexible structures, reduced order system, robustness.**

I. Introduction

THIS paper presents a systematic approach to reduce the order of a model-controller pair for a flexible aircraft. The importance of the controller order reduction problem has motivated researchers to seek solutions that would facilitate the control design procedure, which can be difficult if the model order is high. A reduced-order controller entails a lower computational cost in a real-time implementation. Typically, a reduction is performed on the model and then a controller is designed for the reduced order model. Alternatively, a reduced order controller can be designed based on the full-order model.

The majority of order reduction methods developed so far for linear time-invariant continuous-time systems are carried out in open loop and do not take into account closed-loop stability and performance. The methods of cost analysis [14], balanced reduction [12] and optimal Hankel-norm approximation [7] are some of the most popular in the literature. Some progress was achieved by Enns [5] in his introduction of weighting functions into the classical balanced reduction technique in order to preserve closed-loop stability. Anderson and Liu [1] extended this method to find weighting functions for the controller reduction problem that can maintain closed-loop performance.

The more recent reduction methods guarantee the preservation of closed-loop stability and performance, especially for controller reduction techniques. Goddard and Glover [8] developed sufficient conditions to design a stabilizing reduced order controller achieving a preserved level of performance. This work was based on the following idea: Given a full-order controller K_f achieving the performance level $\gamma := \|\mathcal{F}_L(P,K_f)\|_\infty$ and selecting $\gamma_1 > \gamma$, weighting functions W_1, W_2 are derived such that $\|W_2^{-1}(K_r - K_f)W_1^{-1}\|_\infty < 1 \Rightarrow \|\mathcal{F}_L(P,K_r)\|_\infty < \gamma_1$, where K_r is the reduced order controller, P is the nominal full-order generalized plant model and $\mathcal{F}_L(P,K_r) := P_{11} + P_{12}(I - K_r P_{22})^{-1}K_r P_{21}$ is the lower linear fractional transformation whose $\mathcal{H}_\infty$-norm should be kept small.

All of the above-mentioned order reduction methods do not take into account the physical interpretation of the truncated states. An optimal reduced order model (or controller) may achieve the best level of performance in closed loop, but may only provide limited insight to the engineer if the state vector is no longer in modal form and hence has no direct physical meaning. Our proposed reduction method, inspired from the work of Kavranoglu [9], involves modal truncation, i.e., the truncation of states corresponding to flexible modes of the model. The method then generates an associated reduced order controller satisfying a closed-loop robust performance specification.

Previous research on modal truncation includes the work of Madelaine and Alazard [10], which proposes a model reduction technique based on a frequency-domain heuristic related to the displacement of the effect of the flexible modes in closed loop. In our approach, the main reduction criterion is the achievable closed-loop robust performance level. We use the novel idea of introducing a repeated real parametric uncertainty δ in the flexible modes selected for truncation. This real perturbation, when equal to -1, represents the effect of the truncation of these modes in the aircraft model. Thus, a controller that can maintain some closed-loop performance level for the perturbed full-order aircraft model $\forall|\delta| \leq 1$, can also achieve this robust performance level on the truncated model.

We now describe our reduction procedure. Suppose that it is desired to truncate k flexible modes from the aircraft's full-order model. As a first step, our procedure lists all combinations of k flexible modes from the N flexible modes of the nominal model. This list of mode combinations is shortened by checking specific criteria of robust stability and performance that have to be met. For each candidate combination α of flexible modes to be truncated in the list, a full-order controller $K_{f\alpha}(s)$ is designed and kept in the set $\mathcal{K}_F$ if it achieves the desired robust performance level. Robust performance is measured using the structured singular value with respect to the parametric uncertainty covering the uncertainty in the flexible mode parameters

Manuscript received October 11, 2000; revised July 11, 2001. Manuscript received in final form November 16, 2001. Recommended by Associate Editor J. M. Buffington. This work was supported through research grants from the Natural Sciences and Engineering Research Council of Canada and from the *Fonds pour la formation des chercheurs et l'aide à la recherche du Québec*.

N. Aouf and B. Boulet are with the McGill Centre for Intelligent Machines, McGill University, Montréal, QC, H3A 2A7 Canada (e-mail: boulet@cim.mcgill.ca).

R. Botez is with the Département de Génie de la Production Automatisée, Ecole de technologie supérieure, Montréal, QC, H3C 1K3 Canada.

Publisher Item Identifier S 1063-6536(02)017771-2.

and the truncation of these flexible modes. The result of this first step is the set $\mathcal{K}_F$ of full-order controllers, each one corresponding to a specific combination of flexible modes to be truncated, that meet the desired performance specification both for the full-order aircraft model and its corresponding reduced order model obtained through a truncation of the k modes.

Since the first step in our approach calls for the design of $\binom{N}{k} = N!/(k!(N-k)!)$ full-order controllers, it is limited to aircraft models with up to around 15 flexible modes, depending on computing power and time available for design. Nowadays, it is not unreasonable to assume that a few hours of computations would represent a relatively small cost in the overall design of a new commercial aircraft with flexibilities. What is paramount is to guarantee robust performance with a reduced order controller.

The second step of our procedure consists of generating a reduced order controller for the best full-order controller $\hat{K}_f := K_{f\hat{\alpha}} \in \mathcal{K}_F$ corresponding to mode combination $\hat{\alpha}$. The controller reduction problem is set up as a minimization of the weighted error norm between the nominal closed-loop sensitivity matrix and the reduced one and its solution yields robust performance preservation with the reduced controller. Preservation of robust performance of the reduced model/controller pair is obtained from a structured singular value setup and controller reduction is thus viewed as a robustness problem against uncertainty in the controller. Any controller reduction technique may be used at this stage, as long as the resulting frequency responses of K_r and $\hat{K}_f$ are close enough to ensure that robust performance is preserved with the reduced order controller. We treat both model and controller reduction through the same two-step procedure to obtain a good pair of reduced-order model and controller.

II. Problem Setup

The nominal finite-dimensional linear time-invariant transfer matrix model of a flexible aircraft mapping the control surface inputs u to the measured outputs y, which may be composed of the aircraft's position, angles, linear and angular velocities and accelerations (available to the controller), can be expressed as

$$G(s) = G_{rbm}(s) + G_f(s) \tag{1}$$

where the modal state-space realization of the flexible dynamics $G_f(s)$ is given by

$$G_f(s) = \left[\begin{array}{c|c} A_0 & B_0 \\ \hline C_0 & 0 \end{array}\right] := C_0\,(sI - A_0)^{-1}\,B_0. \tag{2}$$

In this equation, $A_0 \in \mathbb{R}^{2N\times 2N}$ is in modal form, i.e., $A_0 = \mathrm{diag}\{A_i\}$, $A_i = \begin{bmatrix} -\zeta_i\omega_i & \sqrt{1-\zeta_i^2}\omega_i \\ -\sqrt{1-\zeta_i^2}\omega_i & -\zeta_i\omega_i \end{bmatrix}$ $i = 1,\ldots,N$ and N is the number of flexible modes of the model; ζ_i, ω_i are the damping ratio and the undamped natural frequency of the ith mode, respectively; $B_0 \in \mathbb{R}^{2N\times m}$, $C_0 \in \mathbb{R}^{p\times 2N}$. The transfer matrix $G_{rbm}(s)$ models rigid-body dynamics and includes any direct feedthrough terms (D_0 matrix) that might appear in the flexible dynamics. Truncation of the ith flexible mode from the nominal model can be seen as eliminating the effect of this mode. Because there is no interaction between the modal states in the modal realization of $G_f(s)$, this truncation corresponds to setting to zero the 2×2 matrix A_i and the corresponding rows and columns of matrices B_0 and C_0, respectively.

III. Uncertainty Model

Parametric uncertainty may be less conservative than other types of uncertainty and may lead to a more realistic representation of the differences between the dynamics of a flexible aircraft and its model. In our approach, we treat both this kind of uncertainty and the truncation of the corresponding modes through the same setup and with the use of a single repeated real scalar perturbation. Robust performance is optimized against this uncertainty in the design of full-order controllers K_f.

For a desired fixed number of flexible modes to be truncated k, we define the set of all possible combinations of k flexible modes to be truncated as follows:

$$\boldsymbol{a}_k := \left\{\alpha := \{\alpha_1,\ldots,\alpha_N\} : \alpha_i \in \{0,1\}, \sum_{i=1}^{N}\alpha_i = k\right\} \tag{3}$$

where $\alpha_i = 1$ to truncate and $\alpha_i = 0$ to keep the ith mode. For each mode combination $\alpha \in \boldsymbol{a}_k$, we define corresponding perturbations of the modal state-space matrices representing modal parameter uncertainty and the truncation effect of these specific modes. First, let $T_\alpha := \mathrm{diag}\{\alpha_1 I_2,\ldots,\alpha_N I_2\}$. The perturbed plant model is then defined as follows:

$$G_p(s) := G_{rbm}(s) + G_{fp}(s) \tag{4}$$

$$G_{fp}(s) := \left[\begin{array}{c|c} A_0 + \Delta_\alpha^A & B_0 + \Delta_\alpha^B \\ \hline C_0 + \Delta_\alpha^C & 0 \end{array}\right] \tag{5}$$

where the perturbations of the state-space matrices are defined by

$$\begin{bmatrix} \Delta_\alpha^A & \Delta_\alpha^B \\ \Delta_\alpha^C & 0 \end{bmatrix} := \delta \begin{bmatrix} A_\alpha & B_\alpha \\ C_\alpha & 0 \end{bmatrix}, \quad \delta \in \mathbb{R},\ |\delta| \le 1 \tag{6}$$

and the *truncation matrices* A_α, B_α, C_α are given by

$$A_\alpha = T_\alpha A_0, B_\alpha = T_\alpha B_0, C_\alpha = C_0 T_\alpha. \tag{7}$$

The real perturbation δ lies between -1 and 1, covering more than a single objective. The correspondence between values of the parameter δ and the objectives in our design is given as follows:

$$\begin{aligned} &\delta = -1: && \text{Truncate mode combination} \\ &\delta = 0: && \text{Nominal full-order model} \\ &\delta \in]-1,0[\cup]0,1]: && \text{Parametric uncertainty} \\ & && \text{of the truncated modes.} \end{aligned} \tag{8}$$

The latter interval covers variations in the frequencies and damping ratios of the flexible modes to be truncated, as well as their corresponding gains. This uncertainty is useful as the modes truncated from the model are still present (but uncertain) in the aircraft.

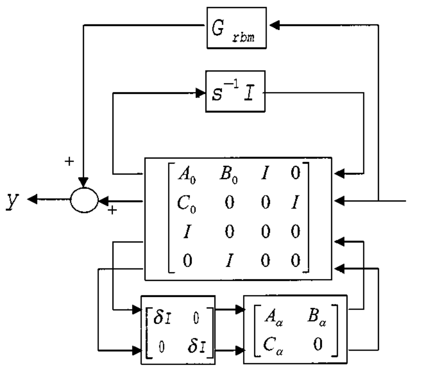

Fig. 1. Parametric uncertainty injection.

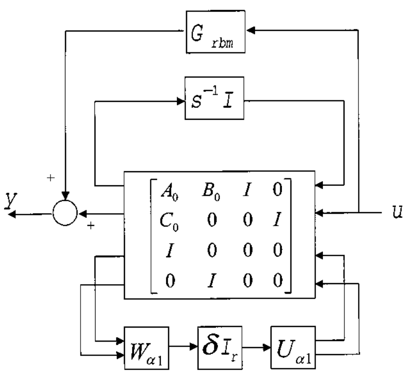

Fig. 2. SVD decomposition of the uncertainty.

The truncation matrices $A_\alpha, B_\alpha, C_\alpha$ are shown on the block diagram of $G_p(s)$ in Fig. 1. In fact, these matrices can be lumped in the augmented plant model. However, the multiplicity of the associated real perturbation δ is high. Using a singular value decomposition of $\begin{bmatrix} A_\alpha & B_\alpha \\ C_\alpha & 0 \end{bmatrix}$, we can reduce the number of repeated perturbations δ, which leads to a less conservative uncertainty model (see [16, Ch. 10])

$$\begin{aligned}\begin{bmatrix} A_\alpha & B_\alpha \\ C_\alpha & 0 \end{bmatrix} &= U_\alpha \Sigma_\alpha V_\alpha^T = [U_{\alpha 1}\ U_{\alpha 2}] \begin{bmatrix} \Sigma_{\alpha r} & 0 \\ 0 & 0 \end{bmatrix} \begin{bmatrix} V_{\alpha 1} \\ V_{\alpha 2} \end{bmatrix} \\ &= U_{\alpha 1} \Sigma_{\alpha r} V_{\alpha 1} = U_{\alpha 1} W_{\alpha 1}\end{aligned} \tag{9}$$

where $r = \operatorname{rank} \begin{bmatrix} A_\alpha & B_\alpha \\ C_\alpha & 0 \end{bmatrix} \leq \max\{2N+m, 2N+p\}$ and $W_{\alpha 1} = \Sigma_{\alpha r} V_{\alpha 1}$. Figs. 2 and 3 show, respectively, how the multiplicity of δ is reduced to r and the matrices $W_{\alpha 1} = [W_{\alpha 11} \quad W_{\alpha 12}]$, $U_{\alpha 1} = \begin{bmatrix} U_{\alpha 11} \\ U_{\alpha 12} \end{bmatrix}$ are incorporated in the augmented plant.

The reduction in the multiplicity of δ yields a less conservative uncertainty set. From Fig. 3, the transfer function between u and y is given by

$$G_p(s) = G_{rbm}(s) + \mathcal{F}_L\left[\mathcal{F}_U(M_\alpha, s^{-1}I), \delta I_r\right]. \tag{10}$$

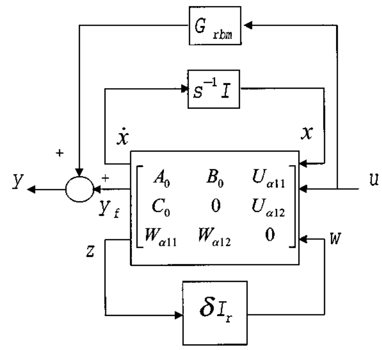

Fig. 3. Augmented plant representation.

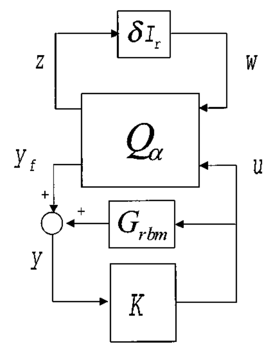

Fig. 4. Robust analysis setup.

where $M_\alpha := \begin{bmatrix} A_0 & B_0 & U_{\alpha 11} \\ C_0 & 0 & U_{\alpha 12} \\ W_{\alpha 11} & W_{\alpha 12} & 0 \end{bmatrix}$ is the real matrix representing the "generalized plant" in Fig. 3. Define the transfer matrix $H_\alpha(s) := \mathcal{F}_U(M_\alpha, s^{-1}I)$ such that

$$\begin{bmatrix} y_f \\ z \end{bmatrix} = H_\alpha(s) \begin{bmatrix} u \\ w \end{bmatrix} \tag{11}$$

where u is the vector of actuator inputs, w is the output of the repeated real perturbation δI_r, y_f is the output of the flexible part of the aircraft's dynamics and z is the input of the repeated real perturbation. Reversing the order of the inputs and outputs of $H_\alpha(s)$, we obtain the augmented plant model $Q_\alpha(s)$, as given by Fig. 4, mapping $\begin{bmatrix} w \\ u \end{bmatrix}$ to $\begin{bmatrix} z \\ y_f \end{bmatrix}$. Fig. 4 represents a typical setup for robustness analysis against a single repeated real perturbation.

Exogenous inputs of interest, e.g., reference signals and disturbances, are grouped together in d and outputs to be controlled, e.g., tracking error and control signals, are grouped in $\tilde{e}$. These signals are added to $Q_\alpha(s)$ together with the performance weighting function $W_p(s)$ such that $e(s) = W_p(s)\tilde{e}(s)$ to obtain the augmented plant model $P_\alpha(s)$ mapping $\begin{bmatrix} w \\ d \\ u \end{bmatrix}$ to $\begin{bmatrix} z \\ e \\ y \end{bmatrix}$. Note that the rigid-body part of the dynamics $G_{rbm}(s)$ is also embedded in $P_\alpha(s)$ using standard block diagram manipulations.

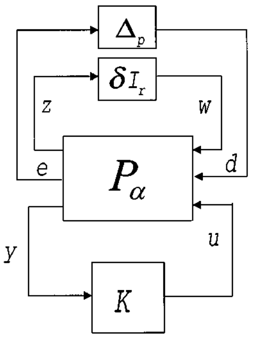

Fig. 5. Robust performance setup.

Fig. 5 shows the μ-synthesis setup for robust performance. The perturbation $\Delta_p \in \mathbb{C}^{n_d \times n_e}$ is a fictitious uncertainty included for performance, linking the exogenous inputs d to the outputs to be controlled e. The uncertainty structure is defined as follows:

$$\Gamma := \left\{ \Delta := \begin{bmatrix} \delta I_r & 0 \\ 0 & \Delta_p \end{bmatrix} : \Delta_p \in \mathbb{C}^{n_d \times n_e}, \delta \in \mathbb{R} \right\} \quad (12)$$

and the corresponding set of stable structured perturbations is defined as

$$\begin{aligned} \boldsymbol{\mathcal{D}}_\Gamma := \{ \Delta(s) \in \mathcal{H}_\infty : & \|\Delta(s)\|_\infty < 1 \\ & \Delta(s_0) \in \Gamma, \forall \mathrm{Re}\{s_0\} > 0 \} . \end{aligned} \quad (13)$$

The perturbed plant model is thus given by $\mathcal{F}_U[P_\alpha(s), \Delta(s)]$, where $\Delta(s) \in \boldsymbol{\mathcal{D}}_\Gamma$.

IV. Model and Controller Reduction

Mixed-μ theory can be used to design a full-order controller achieving the best robust performance index with, e.g., a DGK-iteration or a minimization of $\sup_{\omega \in R} \mu_\Gamma \{ \mathcal{F}_L [P_\alpha(j\omega), K_{f\alpha}(j\omega)]\}$ based on successive $\mathcal{H}_2$ designs [15]. At the end of the first step, we have the set $\boldsymbol{\mathcal{K}}_F$ of full-order controllers which achieve robust performance whether or not the corresponding candidate modes have been truncated.

The second step, after the design of the full-order robust controllers, consists of finding a reduced controller $K_r(s)$ of desired order q from the best full-order controller $\hat{K}_f(s) \in \boldsymbol{\mathcal{K}}_F$ corresponding to the "best" combination $\hat{\alpha}$ of candidate flexible modes to be truncated. Our proposed controller order reduction method preserves robust closed-loop performance, which is not the case for most earlier works. Consider the optimization problem over the set of stabilizing reduced controllers $K_r(s)$ of desired order q

$$\begin{aligned} \inf_{\substack{K_r(s) \\ \text{stabilizing}}} \sup_{\substack{\delta \in R \\ |\delta| \le 1}} & \left\| \mathcal{F}_U \left\{ \mathcal{F}_L \left[P_{\hat{\alpha}}(s), \hat{K}_f(s) \right], \delta I_r \right\} \right. \\ & \left. - \mathcal{F}_U \left\{ \mathcal{F}_L \left[P_{\hat{\alpha}}(s), K_r(s) \right], \delta I_r \right\} \right\|_\infty . \end{aligned} \quad (14)$$

That is, we want the perturbed closed-loop frequency responses with the full-order and reduced order controllers

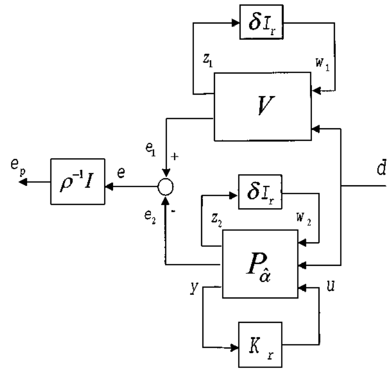

Fig. 6. Controller reduction setup.

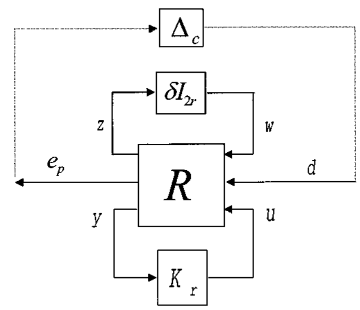

Fig. 7. Augmented plant with the reduced-order controller.

to be as close as possible, as measured by the ∞-norm. A specification can be expressed with $\rho > 0$ as

$$\begin{aligned} & \left\| \mathcal{F}_U \left\{ \mathcal{F}_L \left[P_{\hat{\alpha}}(s), \hat{K}_f(s) \right], \delta I_r \right\} \right. \\ & \qquad \left. - \mathcal{F}_U \left\{ \mathcal{F}_L \left[P_{\hat{\alpha}}(s), K_r(s) \right], \delta I_r \right\} \right\|_\infty \\ & \le \rho, \forall |\delta| \le 1. \end{aligned} \quad (15)$$

Note that ρ should be chosen such that (15) implies robust performance with the reduced order controller. For example, if $\sup_{\omega \in R} \mu_\Gamma [\mathcal{F}_L(P_{\hat{\alpha}}, \hat{K}_f)(j\omega)] = \gamma \le 1$, then one should pick $\rho < 1 - \gamma$. The complex variable s is henceforth dropped to simplify notation. The optimization problem in (14) can be represented as in Fig. 6, where

$$\begin{aligned} \begin{bmatrix} z_1 \\ e_1 \end{bmatrix} &= V \begin{bmatrix} w_1 \\ d \end{bmatrix} \\ V &:= \mathcal{F}_L(P_{\hat{\alpha}}, \hat{K}_f) = \begin{bmatrix} V_{11} & V_{12} \\ V_{21} & V_{22} \end{bmatrix} \end{aligned} \quad (16)$$

This setup can be recast in the robust performance design setup shown in Fig. 7, where $\begin{bmatrix} z \\ e_p \\ y \end{bmatrix} = R \begin{bmatrix} w \\ d \\ u \end{bmatrix}$, $z = \begin{bmatrix} z_1 \\ z_2 \end{bmatrix}$, $w = \begin{bmatrix} w_1 \\ w_2 \end{bmatrix}$, $e_p = \rho^{-1}(e_1 - e_2)$, $R = \begin{bmatrix} R_{11} & R_{12} & R_{13} \\ R_{21} & R_{22} & P_{23} \\ R_{31} & R_{32} & P_{33} \end{bmatrix}$, $R_{11} = \begin{bmatrix} V_{11} & 0 \\ 0 & P_{\hat{\alpha}11} \end{bmatrix}$, $R_{12} = \begin{bmatrix} V_{12} \\ P_{\hat{\alpha}12} \end{bmatrix}$, $R_{13} = \begin{bmatrix} 0 \\ P_{\hat{\alpha}13} \end{bmatrix}$, $R_{21} = [V_{21} \quad P_{\hat{\alpha}21}]$, $R_{22} = V_{22} - P_{\hat{\alpha}22}$, $R_{23} = \hat{\alpha}23$, $R_{31} = [0 \quad P_{\hat{\alpha}31}]$, $R_{32} = \hat{\alpha}32$, $R_{33} = \hat{\alpha}33$. With the inclusion of a fictitious perturbation Δ_c

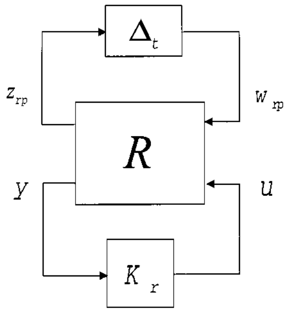

Fig. 8. Uncertainty block augmentation.

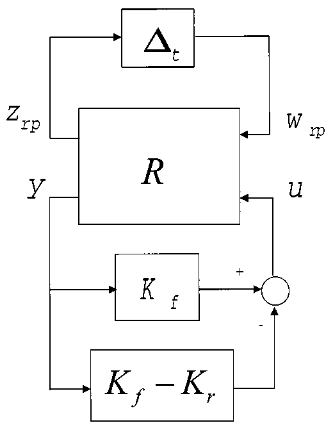

Fig. 9. Introduction of the closeness of the full and reduced controllers.

for the "closeness" performance objective, the final augmented plant is shown in Fig. 8, where $\Delta_t = \begin{bmatrix} \Delta_c & 0 \\ 0 & \delta I_{2r} \end{bmatrix}$. This robust performance controller design can be transformed into a controller reduction procedure by means of robust performance analysis.

From the two equivalent block diagrams shown in Figs. 8 and 9, we obtain in Fig. 10 a robust performance setup in which $\tilde{\Delta}_K := W_K(\hat{K}_f - K_r)$ is viewed as a normalized controller uncertainty, where W_k is a stable scalar weighting function. The idea is to ensure that K_r is close enough to $\hat{K}_f$ such that the size of $\Delta_K(j\omega) = (\hat{K}_f - K_r)(j\omega)$ is within the admissible uncertainty bound for which the system in Fig. 10 will be robustly stable. We use the main loop theorem [13] to prove the following result providing a basis for the proposed controller-order reduction technique. The theorem says that if the reduced order controller is close enough to the full-order controller, then we can obtain both robust performance and closed-loop frequency responses that are close to each other. Define the uncertainty structures as shown in (17)–(18) at the bottom of the page.

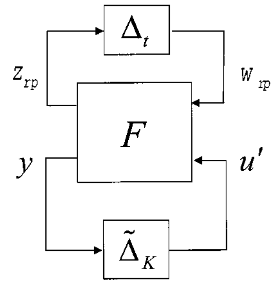

Fig. 10. Augmentation of the plant by adding $\hat{\Delta}_k$ uncertainty.

Theorem 1: Assume that K_f is a full-order stabilizing controller achieving robust performance, i.e., $\sup_{\omega \in R} \mu_\Gamma[\mathcal{F}_L(P, K_f)(j\omega)] < 1$ and assume that the reduced order controller K_r has the same number of unstable poles as K_f. If, for every ω, $\mu_{\Gamma_1}[F(j\omega)] < 1$ and $\|(K_f - K_r)(j\omega)\| \le |W_K^{-1}(j\omega)|$ then we have the following.

1) K_r stabilizes $\mathcal{F}_U[\mathcal{F}_L(P, K_r), \delta I_r], \forall \delta \in \mathbb{R}, |\delta| \le 1$.
2) $\sup_{\omega \in R} \mu_\Gamma[\mathcal{F}_L(P, K_r)(j\omega)] < 1$.
3) $\|\mathcal{F}_U[\mathcal{F}_L(P, K_f), \delta I_r] - \mathcal{F}_U[\mathcal{F}_L(P, K_r), \delta I_r]\|_\infty < \rho, \forall \delta \in \mathbb{R}, |\delta| \le 1$.

Proof: Assume that $\mu_{\Gamma 1}[F(j\omega)] < 1$ and $\|(K_f - K_r)(j\omega)\| \le |{W_K}^{-1}(jw)|$. Then, for any Δ_K such that $K_r = K_f - \Delta_K$ has the same number of unstable poles as K_f and such that $\|\Delta_K(j\omega)\| \le |{W_L}^{-1}(jw)|$, we have $\mu_{\Gamma_2}[\mathcal{F}_L(\mathcal{F}, \tilde{\Delta}_k)(j\omega)] < 1, \forall\omega$ by virtue of the main loop theorem. In particular, taking $\Delta_K = K_f - K_r$ and working our way back to the equivalent system of Fig. 7, we have $\mu_{\Gamma_2}[\mathcal{F}_L(R, K_r)(j\omega)] < 1$ which, by the main loop theorem, implies

$$\|\mathcal{F}_U[\mathcal{F}_L(P, K_f), \delta I_r] - \mathcal{F}_U[\mathcal{F}_L(P, K_r), \delta I]\|_\infty \rho$$
$$< \forall \delta \in \mathbb{R}, |\delta| \le 1.$$

Furthermore, $\forall \delta \in \mathbb{R}, |\delta| \le 1$, we have

$$\begin{aligned} &\|\mathcal{F}_U[\mathcal{F}_L(P, K_r), \delta I_r]\|_\infty - \|\mathcal{F}_U[\mathcal{F}_L(P, K_f), \delta I_r]\|_\infty \\ &\le \|\mathcal{F}_U[\mathcal{F}_L(P, K_r), \delta I_r] - \mathcal{F}_U[\mathcal{F}_L(P, K_f), \delta I_r]\|_\infty < \rho. \end{aligned}$$

Hence

$$\begin{aligned} &\|\mathcal{F}_u[\mathcal{F}_L(P, K_r), \delta I_r]\|_\infty \\ &\le \|\{\mathcal{F}_u[\mathcal{F}_L(P, K_f), \delta I_r] - \mathcal{F}_u[\mathcal{F}_L(P, K_f), \delta I]\}\|_\infty \\ &\quad + \|\mathcal{F}_u[f_L(P, K_f), \delta I_r]\|_\infty < \rho + \gamma < 1. \end{aligned}$$

Finally, the robust stability of $\mathcal{F}_u[\mathcal{F}_L(P, K_f), \delta I_r]$ follows from the main loop theorem and the small-gain condition coming from the argument that the Nyquist plot of

$$\Gamma_1 := \left\{ \Delta := \begin{bmatrix} \delta I_{2r} & 0 & 0 \\ 0 & \Delta_c & 0 \\ 0 & 0 & \Delta_K \end{bmatrix} : \Delta_c \in \mathbb{C}^{n_d \times n_e}, \delta \in \mathbb{R}, \Delta_k \in \mathbb{C}^{m \times p} \right\} \tag{17}$$

$$\Gamma_2 := \left\{ \Delta := \begin{bmatrix} \Delta & 0 \\ 0 & \delta I_{2r} \end{bmatrix} : \Delta_c \in \mathbb{C}^{n_d \times n_e}, \delta \in \mathbb{R} \right\}. \tag{18}$$

$\det[I - K_r\mathcal{F}_U(R,\Delta_t)]$ (Fig. 9) must not be equal to zero, where $K_r = K_f - \Delta_K$ has the same number of unstable poles as K_f (see [4].) ■

To get a reduced controller achieving the specifications, we first proceed as follows. With the use of a fine grid of frequency points, an upper bound $\Psi(\omega)$ on $\|\Delta_K(j\omega)\|$ is found such that the feedback interconnection in Fig. 10 is robustly stable. This is carried out by using, for each frequency ω_i, a bisection technique to find the upper bound $\Psi(\omega_i)$ that leads to $\mu_{\Gamma_1}[F(j\omega_i)] = 1$. Then a fitting procedure can be used to obtain the stable weighting function $W_K(s)$ such that $|W_K{}^{-1}(j\omega)| \cong \Psi(\omega)$. The upper bound $\Psi(\omega)$ is also used as a criterion to reject the mode combinations for which the controller cannot be truncated without losing robust performance. For mode combination α, if $\exists\omega_j$ for which there is no $\Psi(\omega_j) \leq 0$ such that $\|\Delta_K(j\omega_j)\|_\infty \leq \Psi(\omega_j)$ and $\mu_{r_i}[\mathcal{F}_\alpha(j\omega_j)] \leq 1$, then combination α is rejected because the existence of a corresponding reduced order controller satisfying the robust performance specifications cannot be guaranteed. The application of this criterion avoids the need to resort to a heuristic in choosing what subset of mode combinations can be safely truncated.

The last step for controller reduction is the following: Given an order $q < \deg\{\hat{K}_f\}$, find a reduced qth order controller K_r with the same number of unstable poles as $\hat{K}_f$ and such that $\|\hat{K}_f(j\omega) - K_r(j\omega)\| \leq |W_K^{-1}(jw)|$. If such a K_r cannot be found for $\hat{K}_f$, then the second-best full-order controller can be used as a starting point for reduction, i.e., the controller K_f producing the second-to-smallest "μ-norm" $\sup_{\omega\in R}\mu_\Gamma[\mathcal{F}_L(P,K_f)(j\omega)]$ and so forth. Alternatively, the order q may be increased. For this weighted controller approximation problem, any suitable reduction technique can be used, e.g., [1], [5], [7]. In the example below, we used the weighted Hankel-norm approximation because of its close upper bound on the norm of the error between the nominal and the reduced controller. Note that since a μ synthesis may produce an unstable controller, it is suggested that only the stable part be used in the reduction. This ensures that K_r has the same number of unstable poles as K_f and hence Theorem 1 can be used.

A. Modal Reduction Over the Full Flight Envelope of a Flexible Aircraft

For practical flight control applications, one has to keep in mind the changes in aircraft dynamics according to the flight conditions. If these changes can be modeled as slow variations in the modal parameters, one could introduce a suitable complementary uncertainty model capturing these variations for the remaining modes, using for example the technique presented in [2]. Our modal truncation method could then be adapted to yield a reduced order model which, in closed loop, might achieve the robust performance criterion over the entire flight envelope, provided all possible modal parameter variations over the flight envelope could be covered by the complementary uncertainty model. In this case, it might be possible to truncate the flexible modes in such a single-plant model setup. The truncated modes would then represent the less influent modes in terms of performance degradation over the entire flight envelope.

In the case where all possible modal parameter variations over the flight envelope could not be efficiently represented with a structured perturbation connected to a single generalized plant, our reduction method could be applied for different operating points. Each of these frozen operating points would be chosen such that the uncertainties that cover the modal parameters would produce overlapping sets of perturbed plants with the neighboring operating points. After applying our model order reduction technique at each trim point, one could truncate from all aircraft models their shared flexible modes that can be truncated, if this set were nonempty. This truncation of a common set of modes across all models covering the flight envelope would preserve a consistent model structure. The reduced order models could then be interpolated to produce a linear parameter-varying (LPV) reduced-order aircraft model covering the full flight envelope and for which a reduced order scheduling or LPV controller could be designed.

V. Flexible System Example

This example is a flexible system taken from [6], consisting of three masses $m_1 = 11$, $m_2 = 5$, $m_3 = 10$, linked together and to rigid walls through springs of stiffnesses $k_1 = k_4 = 10$, $k_2 = 50$, $k_3 = 55$ and dashpots of viscous dampings $d_i = 0.01k_i$, $i = 1,2,3,4$. The input u is applied such that $f_1 = u, f_2 = 2u, f_3 = -5u$ where $f_i, i = 1,2,3$ are the forces applied on each mass, respectively. The output is $y_1 = 2q_1 - 2q_2 + 3q_3$, where $q_i, i = 1,2,3$ are the mass displacements. A disturbance d, is added to the plant output y_1 to get the system output $y = y_1 + d$. We represented this system in the state-space modal form such that the nominal damping ratios and frequencies, respectively, are: $\zeta_1 = 0.0044$, $\omega_1 = 0.87$, $\zeta_2 = 0.012$, $\omega_2 = 2.43$, $\zeta_3 = 0.025$, and $\omega_3 = 5.12$.

The performance level and the constraint on the controller specified for the nominal model are given by the weighting function $W_p(s) = \begin{bmatrix} (s+3)/(60.5s+0.03) & 0 \\ 0 & 1/0.7 \end{bmatrix}$, which specifies that the closed-loop sensitivity should be smaller than 0.01 at low frequencies. The sensitivity consists, in this case, of the transfer function $T_{dy}(s)$ from the disturbance d to the output of the system y. We start by removing one flexible mode to see if it can be truncated without losing robust closed-loop performance. All three "combinations" of one mode are considered. Table I gives the results obtained for each flexible mode considered for truncation. For the initial design, we selected $\rho = 0.1$, then three full-order controllers of order 28 were designed, with corresponding reduced order controllers of order 11. Note that the relatively high order of the full controllers comes from the use of various weighting functions and scalings in the minimization of the structured singular value to obtain robust performance.

Note that if the condition $\|(\hat{K}_f - K_r)(j\omega)\| \leq \|W_K^{-1}(j\omega)\|$ were satisfied with a reduced order controller with the same number of unstable poles as for $\hat{K}_f$, the performance specification would still be met. Figs. 11 and 12 below represent, respectively, the Bode plots of $\Delta_K(s)$ and $W_K^{-1}(s)$ and

TABLE I
RESULTS FOR TRUNCATION OF A SINGLE FLEXIBLE MODE

	$\max_{\omega_i} \mu_\Gamma[\mathcal{F}_L(P_\alpha, K_{f\alpha})(j\omega_i)]$	$\max_{\omega_i} \mu_\Gamma[\mathcal{F}_L(P_\alpha, K_{r\alpha})(j\omega_i)]$	$\left\|W_K(K_{f\alpha} - K_{r\alpha})\right\|_\infty$
Mode 3	0.7609	0.7609	$<10^{-15}$
Mode 2	1.0928	1.0928	0.0005211
Mode 1	1.0544	1.0544	9.1063×10^{-13}

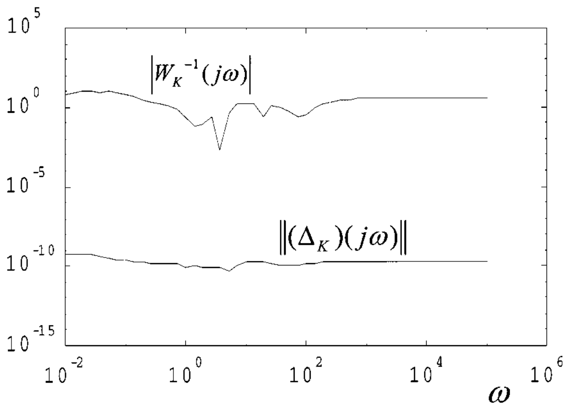

Fig. 11. Norm of Δ_K and magnitude of W_K^{-1}.

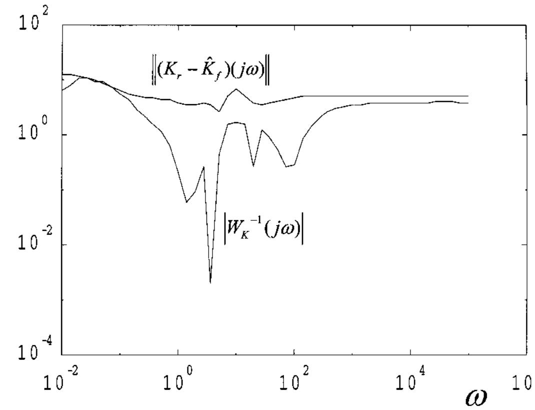

Fig. 13. Norm of $(K_r - \hat{K}_f)$ and magnitude of W_K^{-1}.

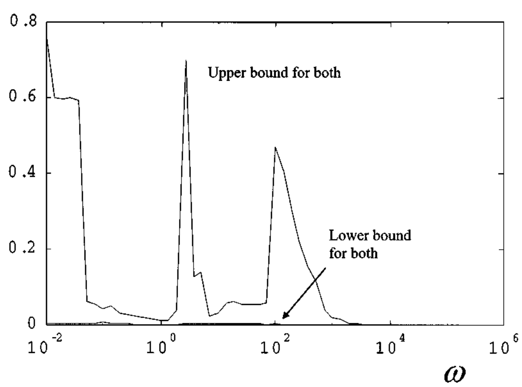

Fig. 12. μ bounds for both full and reduced-order controllers.

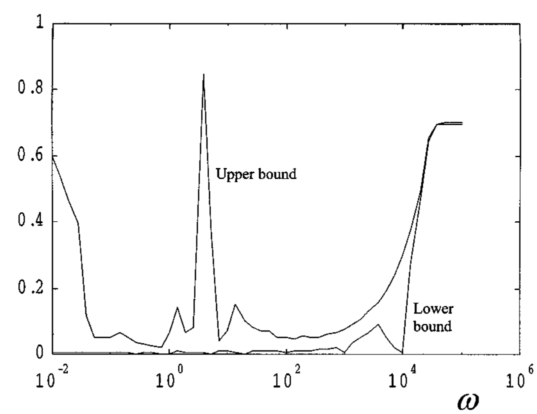

Fig. 14. μ bounds for both full and reduced order controllers.

the upper and lower bounds of $\mu_\Gamma[\mathcal{F}_L(P_3, \hat{K}_f)(j\omega)]$ and $\mu_\Gamma[\mathcal{F}_L(P_3, K_r)(j\omega)]$ for flexible mode 3 truncated.

From the results obtained, we conclude that the best truncation of one mode that we can do is the truncation of mode 3. It satisfies the required specifications of robust performance, both for the full-order and reduced order controllers and the closeness of the corresponding closed-loop sensitivities.

To show the role of the sufficient condition $\|\Delta_K(j\omega)\| \leq |W_K^{-1}(j\omega)|$, we tried to obtain a reduced controller of order 8 with the truncation of mode 3. Fig. 13 shows that this condition was not satisfied. As a consequence, a degradation in performance occurred and we obtained, as shown in Fig. 14, $\max_{\omega_i} \mu_\Gamma[\mathcal{F}_L(P_3, \hat{K}_f)(j\omega_i)] = 0.9851$, whereas $\max_{\omega_i} \mu_\Gamma[\mathcal{F}_L(P_3, K_r)(j\omega_i)] = 0.7609$ as given in Table I.

When we tried to truncate two of the three flexible modes, all three possible combinations considered were discarded because these truncations did not meet the evaluation criteria. The results were as follows:

For combination 1 (mode 2 and mode 3): $\max_{\omega_i} \mu_\Gamma[\mathcal{F}_L(P_1, K_{f1})(j\omega_i)] = 1.87$

For combination 2 (mode 1 and mode 3): $\max_{\omega_i} \mu_\Gamma[\mathcal{F}_L(P_2, K_{f2})(j\omega_i)] = 1.74$

For combination 3 (mode 1 and mode 2): $\max_{\omega_i} \mu_\Gamma[\mathcal{F}_L(P_3, K_{f3})(j\omega_i)] = 1.41$

These truncations did not initially achieve the performance specification with the full-order controllers and obviously with any corresponding reduced order controller. In the case where we relaxed the performance criteria and were willing to accept the performance degradation resulting in the truncation of two flexible modes, the best combination retained by our method was combination 3 (mode 1 and mode 2).

TABLE II
FLEXIBLE MODES

	1	2	3	4	5
ω_i [rd/s]	7.40	15.21	19.73	20.24	38.29
ς_i	0.337	0.056	0.010	0.067	0.023

VI. FLEXIBLE AIRCRAFT EXAMPLE

We illustrate our reduction approach using a flexible model of a B52 bomber [11]. It consists of one short-period rigid-body mode, represented by the angle of attack and the pitch rate and five bending modes taking into account the flexibility of the airframe. The state-space representation of the aircraft is given as

$$\dot{x} = Ax + Bu + B_g w_g \quad (19)$$
$$y = Cx + Du \quad (20)$$

where $x \in \mathbb{R}^{12}$ is the state vector given by, $x^T = [\alpha\ q\ \eta_1\ \dot{\eta}_1\ \eta_2\ \dot{\eta}_2\ \eta_3\ \dot{\eta}_3\ \eta_4\ \dot{\eta}_4\ \eta_5\ \dot{\eta}_5]$, $u = [\delta_{el}\ \delta_{hc}]^T \in \mathbb{R}^2$ is the vector of control surface angles [radians], $y \in \mathbb{R}$ is the vertical acceleration $[g]$, $w_g = [w_{g1}\ w_{g2}\ w_{g3}]^T \in \mathbb{R}^3$ is the vertical gust velocity at three stations along the airplane [m/s], $\alpha \in \mathbb{R}$ is the angle of attack [radians], $q \in \mathbb{R}$ is the pitch rate [radians/s] and η_i is the modal coordinate of the ith mode. The five flexible modes taken into account in the model are characterized by their frequency and damping ratio as given in Table II.

The control objective is to reduce the effect of the wind gusts acting on the aircraft. This can be achieved by regulating the vertical acceleration of the aircraft subjected to these gusts. Using our order reduction procedure, we want to check what flexible mode(s) can be truncated and how much reduction can be performed on the controller while maintaining the robust performance obtained with the original full-order model/controller pair. Thus, we obtain a reduced model/controller pair that maintains the nominal robust performance level. The weighting functions on the acceleration and the control inputs are given by $W_{per}(s) = (40)/(0.05s+1)$ and $W_u = \begin{bmatrix} 1.25 & 0 \\ 0 & 0.25 \end{bmatrix}$, respectively. The weighting function $W_p(s)$ required in our procedure is composed of both $W_{per}(s)$ and $W_u(s)$

Considering the effect of truncating a single flexible mode, we obtained from our reduction technique that the best choice is to truncate mode 1, the lowest frequency mode. The resulting full-order controller $\hat{K}_f = K_{f1}$ was of the 40th-order and it achieved the robust performance level of $\max_{\omega_i} \mu_\Gamma[\mathcal{F}_L(P_1, K_{f1})(j\omega_i)] = 0.9999$. Choosing $\rho = 10^{-4}$, we found that we could reduce the order of the controller down to 18 with $\|W_K(K_r - K_{f1})\|_\infty = 3.0888 \times 10^{-7} < \rho$ and therefore without losing robust performance. Fig. 15 shows the magnitude Bode plots of the two entries of $K_r - K_{f1}$ and of W_K^{-1}, while Fig. 16 shows the mixed-μ bounds for both K_{f1} and K_r (the curves actually sit on top of each other). These figures show that robust closed-loop performance is preserved for the reduced 18th-order controller which also achieved $\max_{\omega_i} \mu_\Gamma[\mathcal{F}_L(P_1, K_{f1})(j\omega_i)] = 0.9999$.

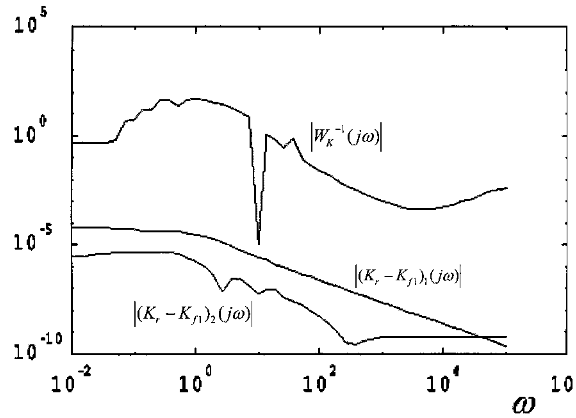

Fig. 15. Magnitudes of the two entries of $(K_r - K_{f1})$ and of W_K^{-1}.

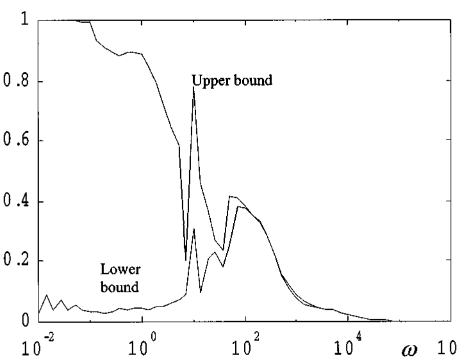

Fig. 16. μ bounds for both full and reduced order controllers.

The other four candidate modes for truncation yielded full-order controllers that could not meet the robust performance specification. Their resulting computed "μ-norms" are given as follows:

$$\begin{aligned} \max_{\omega_i} \mu_\Gamma[\mathcal{F}_L(P_2, K_{f2})(j\omega_i)] &= \max_{\omega_i} \mu_{\Gamma_1}[\mathcal{F}_L(P_4, K_{f4})(j\omega_i)] \\ &= 1.018 \\ \max_{\omega_i} \mu_\Gamma[\mathcal{F}_L(P_3, K_{f3})(j\omega_i)] &= 1.046 \\ \max_{\omega_i} \mu_\Gamma[\mathcal{F}_L(P_5, K_{f5})(j\omega_i)] &= 4.20 \end{aligned} \quad (21)$$

Since robust performance was met with an extremely small margin for the truncation of a single flexible mode, no other flexible mode could be further removed.

VII. CONCLUSION

A systematic model/controller order reduction method for flexible aircraft was presented. The method determines which flexible modes can be truncated from the full-order model of the aircraft and finds a corresponding reduced-order controller preserving robust closed-loop performance. A single repeated real parametric uncertainty for each possible mode combination considered for truncation was adopted. This uncertainty covers both the modal parameter uncertainties and the effect of truncation of these modes from the full-order model. Other sources of uncertainty could be included in the analysis as well. A sufficient condition involving the distance as measured by the

∞-norm between the full-order and reduced order controllers was given to preserve robust closed-loop performance with the reduced order controller. This method is of interest for practical model and controller reduction for flexible aircraft (flexible structure in general) because in this context it is important to keep the physical interpretation of the truncated and remaining modes, without sacrificing robust performance. Future directions on the use of the proposed method for complex, full flight envelope model, and controller reduction problems were discussed. The extension and application of scheduling techniques will be investigated for robust flight control over the full flight envelope of the aircraft.

ACKNOWLEDGMENT

The authors wish to thank the reviewers for their constructive comments.

REFERENCES

[1] B. D. O. Anderson and Y. Liu, "Controller reduction: Concept and approaches," *IEEE Trans. Automat. Contr.*, vol. 34, Aug. 1989.

[2] N. Aouf and B. Boulet, "Uncertainty modeling and complex-rational controller design for flexible structures," in *Proc. AIAA Conf. Guidance, Navigation, Contr.*, Montreal, Canada, Aug. 6–9, 2001.

[3] G. J. Balas, J. C. Doyle, K. Glover, A. Packard, and R. Smith, *μ-Analysis and Synthesis Toolbox*: MUSYN Inc. and The MathWorks, Inc., 1995.

[4] J. C. Doyle and G. Stein, "Multivariable Feedback Design: Concepts for a Classical/Modern Synthesis," *IEEE Trans. Automat. Contr.*, vol. AC-26, pp. 4–16, 1981.

[5] D. Enns, "Model reduction with balanced realizations: An error bound and frequency weighted generalization," in *Proc. 23rd IEEE Conf. Decision . Contr.*, Las Vegas, Dec. 1984, pp. 127–132.

[6] W. Gawronski, *Balanced Control of Flexible Structures*. London, U.K.: Springer-Verlag, 1996, vol. 211, Lecture Notes in Control and Information Sciences.

[7] K. Glover, "All optimal Hankel-norm approximations of linear multivariable systems and their L_∞ bounds," *IEEE Trans. Automat. Contr.*, vol. AC-29, pp. 1115–1193, 1984.

[8] P. J. Goddard and K. Glover, "Controller reduction: Weights for stability and performance preservation," in *Proc. 32nd IEEE Conf. Decision, Control*, vol. 3, 1993, pp. 2903–2908.

[9] D. Kavranoglu, "Controller reduction for uncertain systems," in *Proc. 35th Conf. Decision. Contr.*, Kobe, Japan, December 1996, pp. 887–892.

[10] B. Madelaine and D. Alazard, "Flexible structure model construction for control system," in *Proc. AIAA Conf. Guidance, Navigation, Contr.*, Boston, MA, 1998, pp. 1165–1175.

[11] D. McLean, "Gust load alleviation control systems for aircraft," *Proc. Inst. Elect. Eng.*, vol. 125, no. 7, pp. 675–685, July 1978.

[12] B. C. Moore, "Principal component analysis in linear systems: Controllability, Observability and model reduction," *IEEE Trans. Automat. Contr.*, vol. AC-26, Feb. 1981.

[13] A. Packard and J. C. Doyle, "The complex structured singular value," *Automatica*, vol. 29, pp. 71–109, 1993.

[14] R. E. Skelton, "Cost decomposition of linear systems with application to model reduction," *Int. J. Contr.*, vol. 32, no. 6, pp. 1031–1035, 1980.

[15] C.-D Yang, C.-Y Chang, and Y.-P. Sun, "Mixed μ-synthesis via H_2-based loop-shaping iteration," *J. Guidance, Control, Dyn.*, vol. 21, no. 1, 1997.

[16] K. Zhou, J. C. Doyle, and K. Glover, *Robust and Optimal Control*. Upper Saddle River, NJ: Prentice-Hall, 1996, p. 596.

Nabil Aouf was born in 1972 in Annaba, Algeria. He received the InG (Ingenieur d'etat) degree in automatic control in 1995 and the M.S. degree in electrical engineering in 1997 from Annaba University, Algeria, and Nice University, France, respectively. He is currently pursuing the Ph.D. degree in electrical engineering at McGill University, Montreal, Canada.

He is currently a Consultant for the Industrial Materials Institute of the National Research Council of Canada. His main research interest is related to multivariable robust control with application to aerospace and process systems.

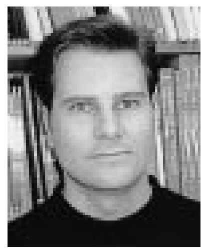

Benoit Boulet (S'88–M'92) was born in 1967 in Saint-Tite, Quebec, Canada. He received the Bachelor's Degree from Université Laval in 1990, the Master of Engineering degree from McGill University, Montreal, QC, Canada, in 1992 and the Ph.D. degree from the University of Toronto, Toronto, ON, Canada, in 1996, all in electrical engineering.

Dr. Boulet is currently Assistant Professor in the Department of Electrical and Computer Engineering at McGill University, where he is Director of the Industrial Automation Laboratory within the McGill Centre for Intelligent Machines. He is president of Coronado Systems, a company specializing in control engineering training and R&D. His research is concerned with finding practical solutions to automation and control problems relevant to industry. His main research areas include manufacturing execution systems, robust industrial process control, robust flight control, and the theory and application of H-infinity control.

Dr. Boulet is a registered Engineer in the province of Quebec, Canada

Ruxandra Botez received the Bachelor's degree in 1984 from the Faculty of Aircraft Construction, Bucharest, Romania, and the Master's degree in 1989 from Ecole Polytechnique de Montreal, Montreal, QC, Canada, with a thesis concerning the semiempirical methods for the dynamic stall prediction on the helicopters. She received the Ph.D. degree from McGill University, Montreal, in 1994 with a dissertation on the chaotic motion of articulated cylinders in annular flow.

She is Associate Professor at Ecole de technologie superieure, Montreal, Canada, since 1998. She acquired five years experience in industrial research at the Factory of Helicopters Construction, Brasov, Romania and at Bombardier Aerospace, Montreal, Canada. Her main area of expertise is aerospace research, more specifically the aeroservoelastic interactions for active control aircraft. Her other areas of interest are flow-induced vibrations, nonlinear dynamics and chaos, aerodynamics, dynamic stall, aeroelasticity, and other fields related to aerospace and mechanical engineering.